Minimization of the kWh cost by optimization of an all-electric chain for the SEAREV Wave Energy Converter.

Judicael Aubry, Marie Ruellan, Hamid Ben Ahmed, Bernard Multon

Minimization of the kWh cost by optimization of an all-electric chain for the SEAREV Wave Energy Converter.

J. Aubry, M. Ruellan, H. Ben Ahmed, B. Multon
SATIE, ENS Cachan Bretagne, CNRS, UEB
av Robert Schuman,
F-35170 Bruz
judicael.aubry@ens-cachan.fr

Abstract

This article presents a two-step approach for the design of a Wave Energy Converter (WEC) electric chain. We show how it is possible, from a bi-objective optimization, to determine the results of several single-objective optimization strategies, in the aim of minimizing the per-kWh production cost. The discussion addresses the influence of operating cycle choice on optimization results, with special attention shown to developing the per-kWh cost of electricity generated.

1. INTRODUCTION

The worldwide energy potential from waves has been estimated at 2,000 TWh/year [1]. Wave energy is derived from a small proportion of wind energy, which itself represents just a small proportion of solar energy. It is however a renewable energy source proves to be particularly consistent in well-exposed coastal areas. Recovering even a small part of this available energy would make a significant contribution to sustainable development efforts. This notion has already served as the source of a large body of work on WEC hydrodynamics as well on power production. The challenge is an interesting one since wave energy recovery offers a unique study context. Wave resources fluctuate considerably and do so on several time scales. Wave period and height provide two quantities that vary over a wide spectrum ranging from seconds to years. WEC design must incorporate this aspect in two distinct ways. First, power take-off (PTO) must be designed so as to withstand such mechanical power fluctuations. For this purpose, moving mechanical parts need to be oversized. Second, the production of fluctuating power is not advisable for the network, making it necessary to devise an approach to smooth the recovered electrical energy. In the case of the well-known Pelamis, energy is stored in high-pressure tanks. Wave Dragon uses the gravitational potential energy of accumulated water as a means of storage.

A direct conversion of the mechanical energy of motion into electrical energy may also be chosen, in which case the discussion turns to direct drive. This pertains to AWS (or Archimedes Wave Swing), which uses a linear electric generator in direct drive [2,3]. The advantage with this type of conversion is to limit both the number of moving parts and the number of energy conversion stages. The risk of failure is reduced, as are maintenance costs. Then an electrical energy smoothing can be performed using electrical storage (e.g. ultracapacitors, etc).

One solution used within the SEAREV[1] system consists of a direct drive implementation of a rotating surface permanent magnet generator, as the rotating topology naturally adapting to the SEAREV movement.

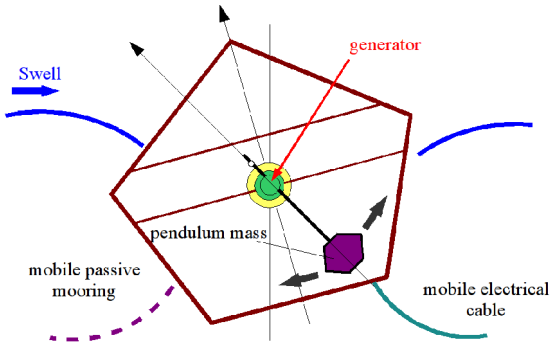

Fig 1: Conceptual diagram of the SEAREV

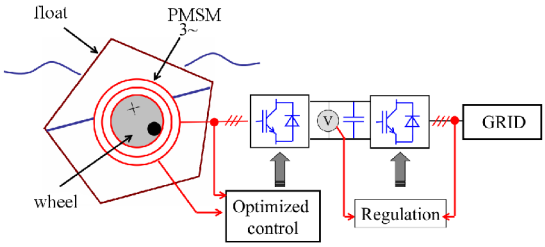

Fig 2: Electric conversion chain

2. THE SEAREV WAVE ENERGY CONVERTER

2.1. Concept and composition

The SEAREV (see Fig 1) consists of a completely enclosed floating body (called the "float") and an embedded pendulum mass ("wheel"). The excitation forces of the wave on the float generate a relative motion between the float and the wheel; this motion in turn is used to recover energy through an electric generator that plays the role of an active damper.

2.2. Hydrodynamic and mechanical modeling

Hydrodynamic and mechanical modeling of the SEAREV was conducted at the LMF Fluid Mechanics Laboratory at the Ecole Centrale de Nantes Engineering School [4]. The SEAREV model used in this study is

1 A French acronym for "système autonome de récupération de l'énergie des vagues" ("Autonomous wave energy recovery system").

indeed linear hydrodynamic yet still includes the non-linearity of pendular wheel movements, which are calculated in a parallel plane to the wave propagation direction. The coupling between hydrodynamics and mechanics is taken into account through the excitation forces as well as through radiation forces, i.e. the forces created by SEAREV movements on its own. From a temporal unidirectional wave profile, this model allows calculating SEAREV movements and in particular the relative motion between wheel and float. Considering that this movement actually drives the generator, the model makes it possible to compute representative generator operating cycles.

The instantaneous wave profile has been reconstructed from the Pierson-Moskowitz spectrum(2.1) [5] which depends on only two parameters that serve to characterize a sea state, namely:

$H_{1/3}$: significant height. This parameter represents the average height among the top third of amplitude observations

T_p : Period within the spectrum corresponding to maximum energy.

We denote herein *S(f)* the energy spectrum and *f* the frequency.

$$S(f)=\frac{A}{f^5}\exp(-\frac{B}{f^4})$$
$$A=\frac{5}{16}\frac{H_{1/3}^2}{T_p^2} \qquad (2.1)$$
$$B=\frac{5}{4}\frac{1}{T_p^4}$$

The N frequency components, spaced by step Δf, which constitutes a computed wave profile (2.2), are generated by the spectrum (2.1) with random phase φ_i.

We shall denote $\eta(t)$ the free surface elevation.

$$\eta(t)=\sum_{i=1}^{N} a_i\cos(2\pi f_i t+\varphi_i) \qquad (2.2)$$
$$with \quad a_i=\sqrt{2S(f_i)\Delta f}$$

In computing many wave profiles for different $H_{1/3}$ and T_p value pairs, we are able to determine the electric generator operating cycles for various sea states.

2.3. Recovery torque control

The damping of relative motion between wheel and float allows for energy recovery. We can summarize the role of the electric generator (damper) as the application of a resistive torque *C(t)* on the wheel, which enables separating the SEAREV electrical model from the hydrodynamic model. On the one hand, the hydrodynamic and mechanical model is considered as a black box with input quantities $H_{1/3}$, T_p and *C(t)* and yielding relative rotational speed between the wheel and float $\Omega(t)$ as its output. On the other hand, an electric and electromagnetic model can be established of the all-electric chain (generator + power electronic converter), with input parameters *C(t)* and $\Omega(t)$, which serves as an operating cycle and enables determining the recovered electrical power over this cycle.

The determination of *C(t)* constitutes an important part of modeling results. For the sake of simplicity, we have decided to correlate *C(t)* and $\Omega(t)$ by means of the following relationship (2.3):

$$C(t)=\begin{cases}\beta\Omega(t) & if \quad \beta\Omega(t)^2\le P_{lev}\\ \dfrac{P_{lev}}{\Omega(t)} & if \quad \beta\Omega(t)^2\ge P_{lev}\end{cases} \qquad (2.3)$$

This expression for the torque applied on the wheel is a linear viscous damping with mechanical leveling power [6]. When mechanical power reaches the value P_{lev}, the viscous damping coefficient β is actually declining in order to maintain the mechanical power constant. While the viscous damping coefficient depends on the sea state, leveling power P_{lev} is held constant throughout the SEAREV life cycle.

The P_{lev} and β values are referred to as control parameters (see Table 2). We can also define these parameters as inputs to the SEAREV hydrodynamic and mechanical model.

2.4. Description of the "all-electric" chain

The modelized generator in this study is a conventional surface permanent magnet synchronous rotating machine, driven by an IGBT PWM converter (2 three-phase bridges, back-to-back on both the machine and network sides) in association with a system that imposes a set of optimized control laws (see Fig 2) [7].

A full description of this electric chain has been provided by a set of 11 parameters detailed in Table 3. A diagram of this generator is displayed in Fig 3.

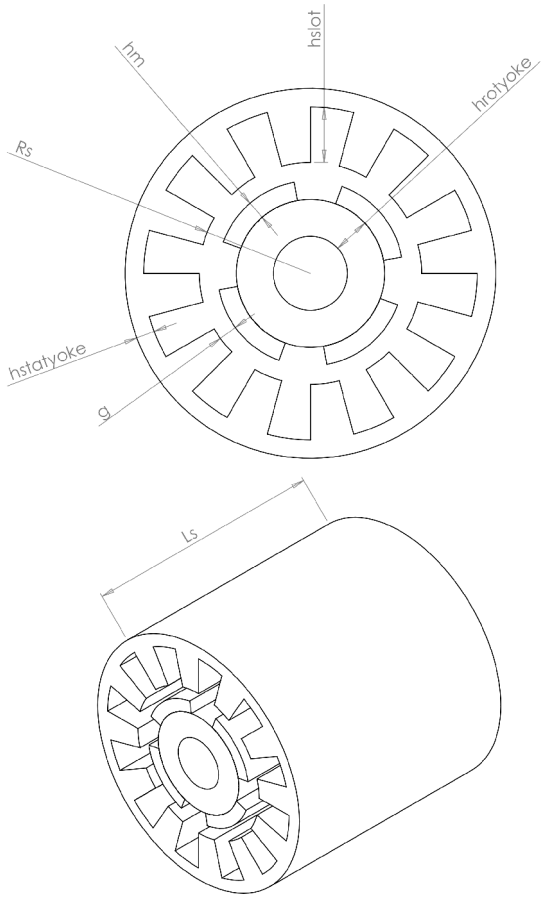

Fig 3: Geometric parameter-based design of the surface permanent magnet synchronous machine

3. OPTIMIZATION METHODOLOGY

The SEAREV device has been designed to convert wave energy into electrical energy. This conversion process must be conducted in optimal fashion, i.e. at greatest efficiency as well as at lowest cost. To achieve these objectives, two possible optimization strategies are available:

- simply minimizing the per-kWh cost on the system operating cycle, which can be achieved by a single-objective optimization. The per-kWh cost is the most significant economic criterion, yet requires knowledge of all system component prices (wheel, float, anchor, mooring, etc.);
- or maximizing the recovered electrical power while minimizing cost, which is achieved through bi-objective optimization.

We shall see in this study that a bi-objective optimization strategy provides direct results for several single-objective optimizations. We start by considering a fixed-geometry SEAREV wheel and float; let's denote C_{Others} the SEAREV cost without an electric chain, C_{elec} and E_{elec} the cost of the electric chain and the recovered electric energy, respectively. The per-kWh cost, denoted C_{kWh}, is expressed by the following expression (3.1)

$$C_{kWh} = \frac{C_{elec} + C_{Others}}{E_{elec}} \qquad (3.1)$$

The contradiction between the two objectives C_{elec} and E_{elec} allows postulating the existence of a Pareto front, which may be written in the form of the monotonous and, in this instance, increasing $C_{elec}(E_{elec})$ function. The point on this front that minimizes the per-kWh cost also verifies relationship (3.2):

$$\frac{\partial C_{kWh}}{\partial E_{elec}} = 0 \quad for \quad C^*_{elec}(C_{Others}) = \frac{\partial C_{elec}}{\partial E_{elec}} E^*_{elec} - C_{Others} \qquad (3.2)$$

The point on this front that verifies this relationship has a tangent passing through the point $(0,-C_{Others})$ in the (E_{elec},C_{elec}) plane.

While a single-objective optimization, i.e. minimizing the per-kWh cost, would be needed for each value C_{Others}, a bi-objective optimization enables, after a post-calculation analysis, determining the minimum per-kWh cost C_{kWh}*, as a function of any value of C_{Others}. It also becomes possible to identify the maximum SEAREV cost (without the electric chain and for a fixed geometry) to ensure system profitability, depending on the per-kWh redemption price.

To achieve bi-objective optimization, we have used a stochastic method. The diagram of this optimization is shown in Fig 5, and the method requires computing the entire SEAREV model several times. During the model resolution phase, the hydrodynamic and mechanical step actually proves to be the most time-consuming. For a given sea state, computing the $[C(t),\Omega(t)]$ cycle over a 2000 s time horizon takes about 40 seconds (Pentium IV, 3.2 GHz, Windows XP).

As part of an optimization strategy with a dozen or so optimization parameters, the typical number of objective function evaluations is approximately 100,000, which amounts to a month and a half of computing time for a single optimization! It is also well known that in order to verify the convergence, several restarts are necessary. The overall computing time needed to optimize SEAREV is therefore totally unacceptable.

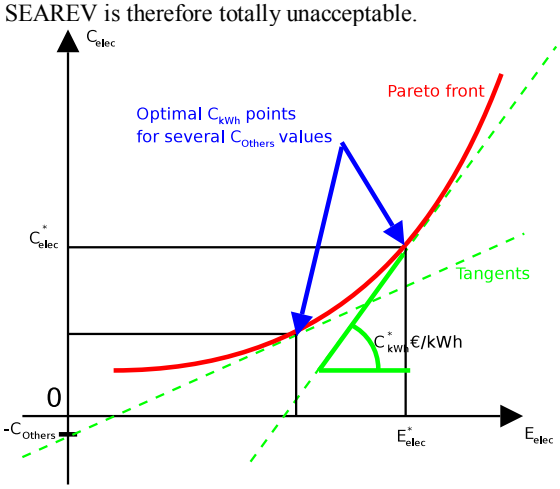

Fig 4: C_{kWh} minimization according to a bi-objective (E_{elec},C_{elec}) optimization

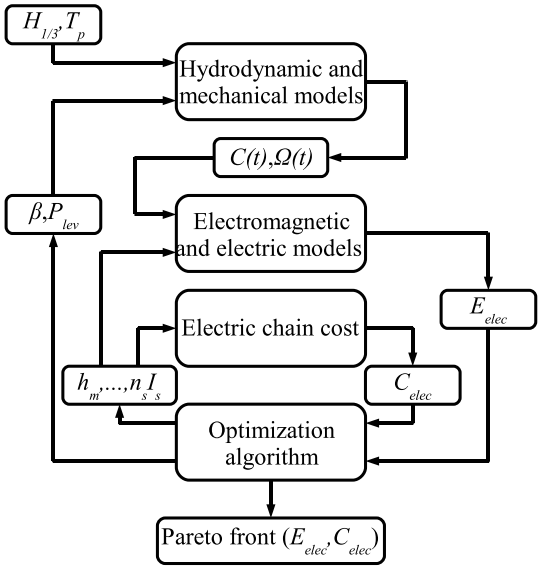

Fig 5: One step optimization, parameters on the left, objectives on the right.

In order to reduce computing time, the solution adopted consists of performing two successive optimizations. The first contains just a few parameters and thus features only a few evaluations of objectives; this optimization involves the hydrodynamic and mechanical model. The second, including a greater number of parameters, no longer needs to incorporate this part of the model. The choice of parameters and objectives for each optimization must be consistent. Our selection comprises:

For this first optimization, we have chosen optimization parameters P_{lev} and β, i.e. the control parameters (see Table 2). The objectives of this optimization are to maximize the recovered mechanical energy and minimize the highest mechanical power over the cycle. These two objectives are assumed on an *a priori* basis to be helpful for the second optimization objectives.

These are indeed to maximize the recovered electrical power over a cycle and minimize the cost of electric chain. The parameters serve to describe the electric chain (see Table 3). This optimization should be conducted

over a complete operating cycle, to be selected following the first optimization. The explanation herein is limited to calculation of the electric chain cost. A full explanation of the recovered electrical energy calculation entails complex and lengthy developments of electric chain modeling [7]. Let's simply note that this energy is in fact the mechanical energy of the cycle $[C(t),\Omega(t)]$, less losses. We are considering both Joule and magnetic losses, however, the losses in power electronic converter and mechanical losses have not been taken into account.

$$C_{elec} = C_{generator} + C_{converter} \quad (3.3)$$

$$C_{generator} = M_{Fe} C_{Fe} + M_{Cu} C_{Cu} + M_{magnet} C_{magnet} \quad (3.4)$$

$$C_{converter} = 6.4 (S_{converter})^{0.7} \quad (3.5)$$

with $S_{converter}$ being the converter apparent power expressed in VA.

C_{elec} equals the sum of the cost of materials (see Table 4) needed to build the generator plus the converter cost. Due to a lack of data, the cost of inactive materials and manufacturing costs have not been included. The relationship (3.5) stems from a widespread data collection effort.

Moreover, we are imposing some physical and geometric optimization constraints:

- Temperature constraint: Heating of the generator, as calculated from the average value of losses, should not exceed 135°C;
- Operating constraint: All points on the cycle should be reachable by the electric chain and must respect the saturation, demagnetization, voltage and current constraints.
- Geometric constraint: Limit feasibility at the rotor.

The diagram of this two-step optimization is presented in Fig 6.

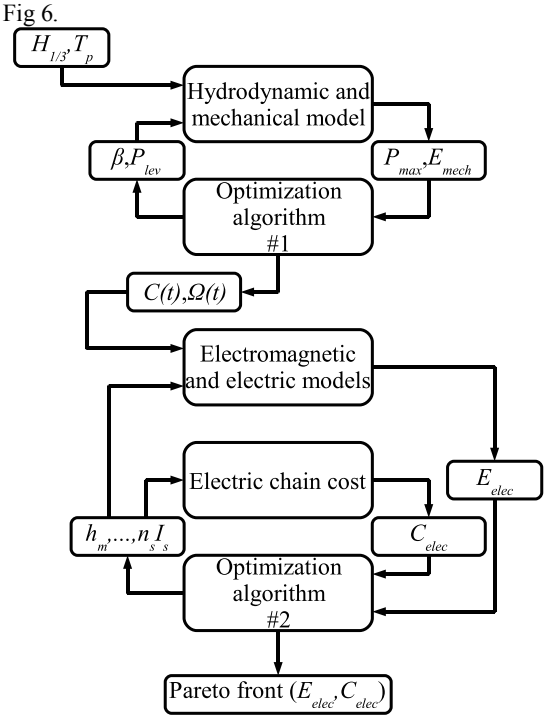

Fig 6: Two-step optimization, parameters on the left, objectives on the right.

4. OPTIMIZATION RESULTS

4.1. First step

This optimization consumes more computing time. We have chosen to undertake a systematic calculation; the number of parameters is low and we can discretize these variables and calculate the objectives associated with all the created points. The mesh size is 40*40, i.e. a total of 1,600 points representing 18 hours of computation time. This step has been performed for a sea state $H_{1/3}$ = 3m and T_p = 8 s.

Figure 7 shows the isovalues of mechanical energy vs. viscous damping coefficient and leveling power.

For a given leveling power, the value of the mechanical energy as a function of the viscous damping coefficient increases first before decreasing. A specific coefficient value serves to maximize the recovered mechanical energy. For a given damping coefficient, the recovered mechanical energy value is an increasing function of leveling power and tends towards a limit. Leveling power actually limits the available power conversion, but above a given value, leveling is rarely achieved on the cycle and its influence on total recovered energy becomes very weak.

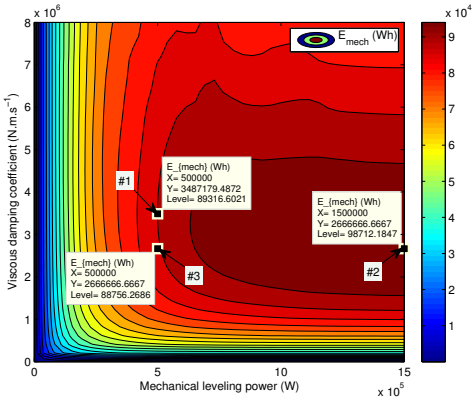

Fig 7: Mechanical recovered energy (Wh) vs. β, the viscous damping coefficient, and P_{lev}, the leveling power, for a sea state $H_{1/3}=3m$ and $T_p=8s$.

Figure 8 shows the isovalues of the P_{ave}/P_{max} ratio, also versus P_{lev} and β. This ratio reflects the necessary power oversizing of the electric chain in comparison with average mechanical power provided by the cycle. As the leveling power rises, this ratio becomes lower.

This systematic calculation offers sufficient information on the influence of parameter control towards meeting the objective. A set of optimal solutions distributed on a Pareto front (see Fig. 9) can be easily generated. We first noticed on this front the presence of a recoverable mechanical energy limit, i.e. near 99kWh for our case. This value is reached when leveling power is such that actual leveling can never be attained.

We have also noted the possibility of reducing the maximum mechanical power by 60% (up to 500 kW) while only lowering the recovered mechanical energy by 10% (from 99 to 89 kWh).

Figure 10 displays the Pareto set within the parameter space (P_{lev}, β). When it is sought to reduce leveling power, the viscous damping coefficient must be increased accordingly in order to recover the greatest amount of energy.

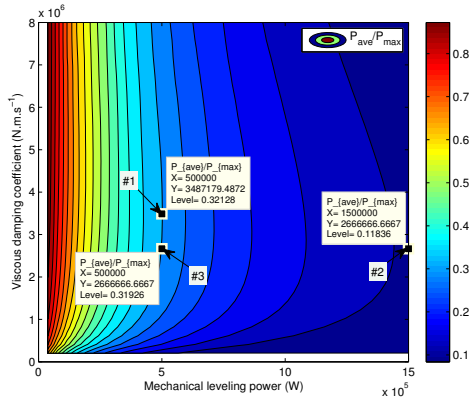

Fig 8:P_{ave}/P_{max} ratio vs. β, the viscous damping coefficient, and P_{lev}, the leveling power, for a sea state $H_{1/3}$=*3m* and T_p=*8s*.

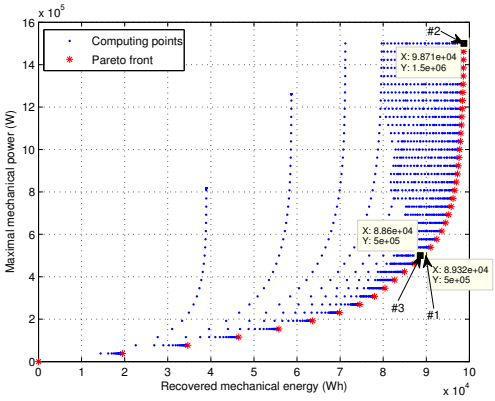

Fig 9: Computing points within the objective plane (E_{mech},P_{max}) and the corresponding Pareto front

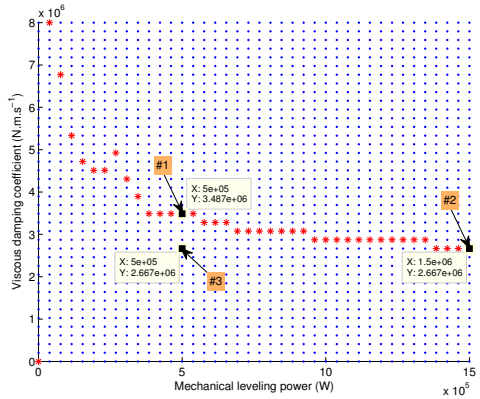

Fig 10: Computing points in the parameter space (P_{lev},β) and corresponding Pareto set

This systematic study is not an optimization algorithm by itself, but rather yields reliable results at low computation times. If a stochastic algorithm had been used, the number of objective evaluations would have been at least 1,600. However, several restarts were needed to verify algorithm convergence.

From this stage, three configurations with different sets of control parameter values (listed in Table 1) have been retained for the purpose of highlighting the influence of operating cycle choice on electric chain design.

Configurations #1 and #2 are both located on the Pareto front, with configuration #1 displaying a lower leveling power (500 kW) than #2 (1,500 kW), which is located at the far right of the front. Configuration #3 has the same leveling power as #1 but a different damping coefficient β. The recovered mechanical energy for these two points is very similar.

Table 1: The set of selected control parameter configurations

N°	β (N.m.s^{-1})	P_{lev} (kW)	E_{meca} (kWh)	P_{ave}/P_{max}
#1	3,5.10^6	500	89,3	0,32
#2	2,67.10^6	1500	98,7	0,12
#3	2,67.10^6	500	88,7	0,32

4.2. Second step: Electric chain optimization.

4.2.1. Optimization algorithm

The system to be simulated requires a complex modeling set-up, as it entails optimizing two objectives that depend on 11 design parameters. We have opted to use an algorithm based on particle swarm [8]. For each optimization, the number of particles equals 1,000 with an archive size (i.e. set of solutions stored at each iteration) of 100 for 1,300 iterations. In order to obtain viable solutions economically, we have limited the electric chain cost to a value of € 2M, which allows defining the Pareto front more precisely in the area of greatest interest to this study.

4.2.2. Results

Figure 11 presents the Pareto fronts obtained at the end of optimization for the three selected control parameter configurations. The two goals are contradictory: increasing conversion efficiency implies increasing the electric chain cost and particularly the generator cost. It is known that generator losses will be even smaller at a greater mass, hence at higher cost.

The apparent power, and thus the cost of the power electronic converter (see Eq. 3.5), remains relatively constant along the front (Fig. 12).

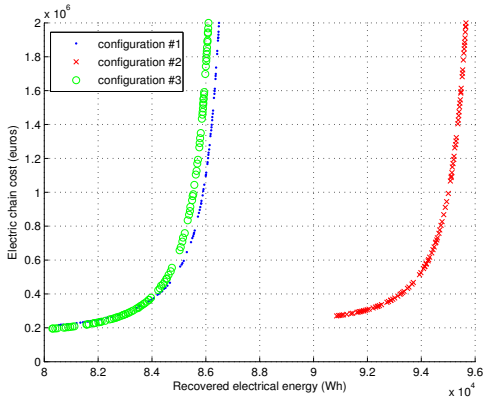

Fig 11: Pareto fronts

The apparent power of the converter is always slightly greater than the leveling power due to the impossibility of obtaining a unity power factor ($cos(\varphi)$) on all points of the cycle.

We can observe on these fronts that configuration #2 (P_{lev} = 1,500 kW) yields more electrical energy on the

cycle. The mechanical energy potential is in fact higher: 98 kWh vs. 88 kWh for configuration #1. In contrast, it is not possible to obtain electric chain costs below € 270k, while the most economical solutions for configuration #3 reach € 195k. The constraint limiting the evolution of fronts to an even lower cost would be the heating constraint. On the left of the front, conversion efficiency does indeed drop and energy losses increase, thereby creating a temperature rise in reaching the constraint.

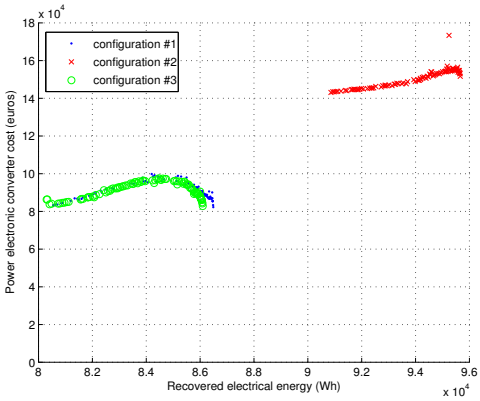

Fig 12: Cost of the power electronic converter along the Pareto front

For configurations #1 and #3, a difference is once again observed in the mechanical energy potential. The two corresponding fronts are relatively close to one another and intersect at around € 330k. Above this cost, configuration #1 is the most advantageous and below it, #3 becomes the most prudent in seeking to minimize electric chain costs.
Configuration #3, which was not on the Pareto front in the first step, leads to solutions offering lower costs than the other two configurations and that are therefore Pareto optimal.

5. ELECTRIC per-kWh COST ANALYSIS

To determine the per-kWh cost provided by the electrical system, the electrical energy produced during the system life cycle (typically 20 years) must be known. To calculate this energy amount with precision, a representative system operating cycle needs to be built from several different sea states and from their probabilities of occurrence on a given sea site. Since control parameters pertinent for one sea state are not necessarily so for another state, the construction of such a cycle requires optimizing these parameters for each sea state. In this study, we will adopt the simplifying assumption that SEAREV is subject to a single sea state for a 20-year period, specifically the state $H_{1/3}$=3 m and T_p=8 s for which the optimization has so far been conducted, which is a rather powerful sea state. This assumption prevents us from proceeding with a quantitative study, yet offers a purely methodological step towards a more comprehensive optimization. The comparisons drawn remain within a general realm. Figure 13 shows the minimum per-kWh cost values for several C_{Others}, i.e. the SEAREV cost without any electric chain. These results are based on the Pareto fronts given in Figure 11. C_{kWh} increases with C_{Others} due to a rise with investment. In Figure 4, we can note that as the point (0,-C_{Others}) decreases, a higher slope is found for the Pareto front tangent. This slope is nothing more than the minimum cost C_{kWh} corresponding to the C_{Others} value.
It is worthwhile to observe that below € 400k for C_{Others}, configuration #3 shows the lowest per-kWh cost. This solution, which did not lie on the Pareto front of the first step, is of interest over a range of C_{Others}. Beyond this range, configuration #2 features the lowest C_{kWh} cost. The gain in electrical energy thanks to greater leveling power offsets the additional investment on the electric chain only if the SEAREV cost without an electric chain exceeds € 400k. Configuration #1 is not attractive in comparison with the other two, and this point was even located on the Pareto front of the first optimization step.

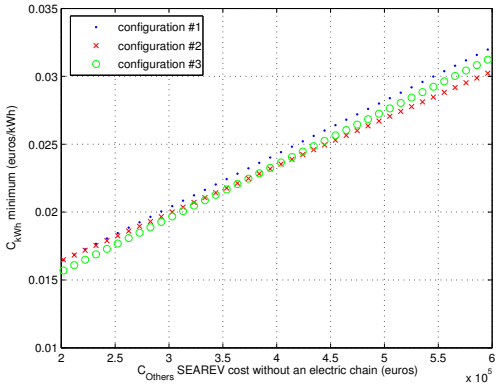

Figure 13: Minimum C_{kWh} vs. C_{Others}

6. CONCLUSION

We first presented a methodology for optimizing the design of an "all electric" chain for a wave energy converter. A two-step approach was adopted, not for the sake of simplification, but instead over computing time concerns. The first stage involves the optimization of control parameters for the recovery torque and is presumed to enable choosing an optimal cycle for designing the electric chain during a second optimization step. We then examined the sensitivity of results to the choice of control parameter configuration. It was found that an optimal cycle at the end of the first stage is not necessarily still optimal at the end of the second stage. The leveling of recovered mechanical power, which *a priori* offers an attractive solution to avoid oversizing the electric chain (particularly the power electronic converter), was studied in terms of the per-kWh electric cost. The advantage of this solution depends heavily on the SEAREV cost without an electric chain. In order to minimize the per-kWh electric cost, it is necessary to choose leveling power in accordance with this fixed cost.

This study should now be extended, notably by calculating the recovered electrical energy over a representative cycle of the system life cycle, hence with several sea states. Other types of control must be studied as well, particularly Latching control [5,9], which has a poor P_{ave}/P_{max} ratio yet still allows recovering more mechanical energy. The scale effect on SEAREV geometry may be a determining factor in minimizing the per-kWh cost. A study of this issue could instruct whether it is better to increase the number of SEAREV or increase its size.

7. APPENDIX : NOTATIONS

Table 2: Control parameters of the recovery torque

Parameter	Definition
β	Viscous linear damping coefficient
P_{lev}	Mechanical leveling power

Table 3: "All-electric" chain parameters

	Parameter	Definition
Generator	h_m	Magnet height
	L_s	Useful generator length
	p	Number of poles pairs
	h_{slot}	Slot height
	$h_{rotyoke}$	Rotor yoke height
	$h_{statyoke}$	Stator yoke height
	R_s	Internal stator radius
	g	Air gap length
	k_{CuFe}	Proportional coefficient between iron and copper in the slotting area
Converter	$(\frac{V}{n_s})$	Nominal r.m.s per turn voltage of the converter
	$n_s I_s$	Nominal r.m.s. amperes turns of the converter

Table 4: Raw materials per kg cost

Material	C_x = *per kg cost, in* €/kg
Iron	3
Copper	6
Magnet (NdFeB)	30

Table 5: Economics and energy notations

Notation	Definition
C_{elec}	Electric chain cost
C_{Others}	SEAREV cost without an electric chain
C_{kWh}	per-kWh production cost
$C_{generator}$	Generator cost
$C_{converter}$	Power electronic converter cost
E_{mech}	Recovered mechanical energy
E_{elec}	Recovered electrical energy

8. REFERENCES

[1] Thorpe T., (2007). "Wave Energy" chap 14 of 2007 Survey of Energy Ressources, World Energy Council, pp 543-549

[2] Polinder H., Damen M.E.C., Gardner F., (2004). "Linear PM Generator System for Wave Energy Conversion in the AWS", IEEE Transactions on energy conversion, vol 19, n° 3, september 2004

[3] Mueller M.A., (2002). "Electrical Generators for Direct Drive Wave Energy Converters", in IEEE proceedings Gener. Transm. Distrib., Vol 149, n°4, july 2002

[4] Babarit A., (2005). "Optimisation hydrodynamique et contrôle optimal d'un récupérateur de l'énergie des vagues", PhD thesis, Ecole Centrale de Nantes.

[5] Falnes J., (2002). "Ocean Waves and Oscillating Systems", Cambridge University Press.

[6] Ruellan M., Ben Ahmed H., Multon B., Babarit A., Clément A.C., (2006). "Control Influence on the Electromagnetic Generator Pre-Design for a Wave Energy Converter", In Conf ICEM 2006

[7] Ruellan M., (2007). "Méthodologie de dimensionnement d'un système de récupération de l'énergie des vagues", PhD Thesis, École Normale Supérieure de Cachan

[8] Engelbrecht A.P., (2005). "Fundamentals of Computational Swarm Intellingence", Wiley

[9] Babarit A., Duclos G., Clément A.H., (2005). "Comparison of latching control strategies for a heaving wave energy device in random sea", Applied Ocean Research 26, pp 227-238, Elsevier.